A note on Stokes phenomenon in flow under an elastic sheet

Christopher J. Lustri[1]*, Lyndon Koens[1], Ravindra Pethiyagoda[2]

[1]Department of Mathematics and Statistics, 12 Wally's Walk, Macquarie University, New South Wales 2109, Australia
[2]School of Mathematical Sciences, Queensland University of Technology, Brisbane QLD 4001, Australia

Abstract

Stokes phenomenon is a class of asymptotic behaviour that was first discovered by Stokes in his study of the Airy function. It has since been shown that Stokes phenomenon plays a significant role in the behaviour of surface waves on flows past submerged obstacles. A detailed review of recent research in this area is presented, which outlines the role that Stokes phenomenon plays in a wide range of free surface flow geometries. The problem of inviscid, irrotational, incompressible flow past a submerged step under a thin elastic sheet is then considered. It is shown that the method for computing this wave behaviour is extremely similar to previous work on computing the behaviour of capillary waves. Exponential asymptotics are used to show that free-surface waves appear on the surface of the flow, caused by singular fluid behaviour in the neighbourhood of the base and top of the step. The amplitude of these waves is computed and compared to numerical simulations, showing excellent agreements between the asymptotic theory and computational solutions.

1 Introduction

Stokes phenomenon was discovered by George Gabriel Stokes in his analysis of the Airy function [42, 43]. It was well-known that the Airy function has oscillatory behaviour for large negative values, and decays exponentially for large positive values. Stokes explored how this behaviour arises by studying the asymptotic behaviour of the Airy in the complex z-plane for large $|z|$ along paths connecting the oscillatory and exponentially decaying regions. In doing so, Stokes found something remarkable; there exist curves in the complex plane across which exponential terms seem to appear out of nowhere. Capturing this asymptotic behaviour required very careful calculation by Stokes, as the terms are exponentially small in the limit that $|z|$ becomes large, and so are invisible to classical asymptotic power series methods. The behaviour Stokes identified was subsequently termed "Stokes phenomenon", and the special curves across which exponentials switch on or off became known as "Stokes curves".

The switching associated with Stokes phenomenon in singularly perturbed problems is exponentially small in the asymptotic limit, and therefore new asymptotic techniques known were required in order to fully capture this switching behaviour. Berry [7, 6, 8] and Berry & Howls [9, 10] established the a divergent asymptotic series may be truncated optimally in order to approximate an exact solution, and that the error of this approximation is exponentially small in this limit. Hence, rescaling the problem to examine this truncation error allows for direct asymptotic study of these exponentially small terms. This idea was used to develop new asymptotic methods for studying exponentially small behaviour, known as exponential asymptotics, asymptotics-beyond-all-orders, or hyperasymptotics.

Berry used this idea to study Stokes curves in the Airy function [6]. This study found that the switching us smooth, and occurs in a local neighbourhood in the vicinity of the Stokes curve. These ideas have subsequently found a huge range of applications, including crystal growth [27], astrophysics [2], and string theory [3], among many others. In particular, Stokes curves have been found to play a significant role in many singularly-perturbed water wave problems. Early work on this topic studied gravity-capillary waves

*Electronic address: christopher.lustri@mq.edu.au

modelled using singularly-perturbed variants of the Korteweg-de Vries (KdV) equation [1, 12, 23, 22, 44, 41]. Chapman & Vanden-Broeck subsequently used exponential asymptotics to study two-dimensional nonlinear gravity waves [16] and capillary waves [15]. These two studies led into a number of works that applied related techniques to study other geometries [31, 32, 45, 49, 48], gravity-capillary waves [46, 47], and waves in three dimensional domains [29, 30, 33]. These studies will be reviewed in more depth in Section 1.1.

In this paper, we add to these results by considering the problem of flow past a submerged obstacle, under an infinitely-thin elastic sheet. Elastic sheets on a fluid are often used as a model for flow past an ice sheet, and a very substantial number of previous studies on this topic exist. Many previous studies considered flexural-gravity waves, typically considering solitary or periodic waves. See, for example, the computational and asymptotic studies in [5, 19, 20, 24, 34, 35, 37, 50]. For a more comprehensive review of this area, see [38]. The present study does not consider solitary or period wave configurations, but rather the behaviour of waves in an elastic sheet caused by steady flow over submerged obstacles.

In this study, we use an exponential asymptotic method developed by Chapman, King & Adams [13] for studying Stokes curves in nonlinear differential equations. This technique extends upon an earlier method by Olde Daalhuis et al. [36] for studying Stokes curves. The method will be described in Section 1.2. The process for determining the amplitude of waves on the elastic sheet is extremely similar to finding the amplitude of capillary waves using exponential asymptotics in [15]. We therefore follow a very similar method to show how Stokes phenomenon produces elastic free-surface waves. We determine that there are two wave contributions present downstream from the obstacle which are switched on across Stokes curves, and find the amplitude of the downstream wavetrain. Finally, we suggest a number of interesting future directions arising in the study of flow past elastic sheets.

1.1 Stokes phenomenon in Water Wave Problems

The earliest studies into the behaviour of water waves using exponential asymptotics came about when a number of authors noticed that singularly perturbed variants of the KdV equation typically produced solutions with qualitatively important and distinct behaviour on exponentially small scales [1, 12, 41]. In particular, a number of studies considered the behaviour of travelling waves in the singularly perturbed fifth-order KdV equation [22, 23, 44]. While the non-perturbed KdV system typically contains solitary wave solutions, these studies found that the corresponding solutions for the fifth-order KdV are not true solitary waves. Instead of being exponentially localised, these travelling waves possess an exponentially small train of oscillations that extends indefinitely from the main wave core without decaying. These oscillations were found to switch on across Stokes curves in the analytically-continued solution which allowed the amplitude of these waves to be determined.

A significant breakthrough came about through the work of Chapman & Vanden-Broeck [15, 16]. In first of these papers, the authors studied capillary waves caused by inviscid, irrotational, incompressible (potential) flow past a submerged obstacle with small surface tension. In the second, the authors studied gravity waves with small Froude number in the same geometry. In both cases the downstream waves cannot be captured by an asymptotic power series, as they are exponentially small in the asymptotic limit. The authors devised a strategy which involved expressing the flow in the complex potential plane in terms of the fluid potential (ϕ) and the streamfunction (ψ), shown in Figure 1. This has the effect of mapping the free boundary to a known curve. The procedure then involves analytically continuing the free surface downwards, and identifying Stokes curves in this analytically continued domain. A schematic of this process, also used in the current study, is seen in Figure 2. The authors then performed an exponential asymptotic analysis of these Stokes curves, and were able to compute the amplitude of these exponentially small waves in the far field.

These results clearly showed that exponential asymptotics would be a valuable tool for computing water wave behaviour in various limits, and inspired a number of studies which aimed to extend the picture laid out in [16, 15]. Immediate extensions involved analysis of flow in new two-dimensional geometries, such as the work of [31, 32]. The first of these studies calculated the behaviour of waves caused by flow past ridges and trenches, identifying configurations which produced trapped waves, or waves restricted to a localised region. The second resolved some open questions arising in [16] regarding the waves caused by flow due to a submerged source. Other works considered the effects of surface-piercing obstacles such as waves caused by single [49] and multi-cornered hulls [48], which led to theoretical advances that link Stokes phenomenon

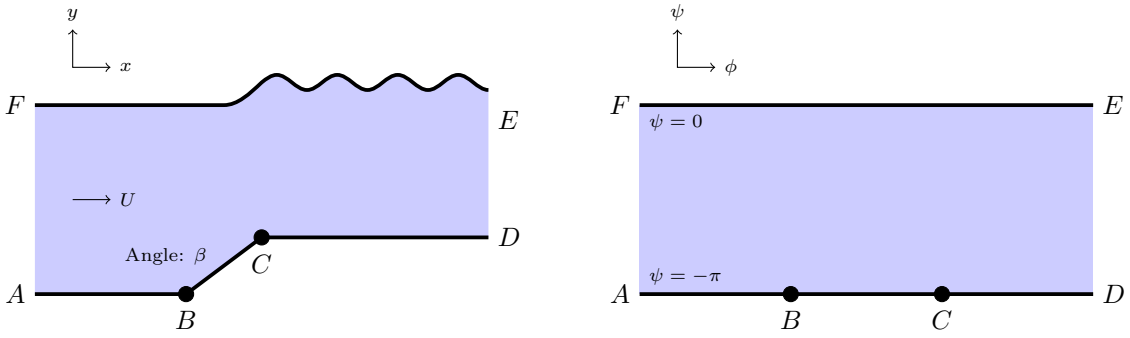

(a) Physical Fluid Domain: $z = x + \mathrm{i}y$ (b) Complex Potential Domain: $w = \phi + \mathrm{i}\psi$

Figure 1: Mapping of a fluid domain to a fixed known region of the complex potential plane. Steady flow follows streamlines, which are curves in the potential plane with constant ψ. The free surface maps to the top streamline, typically labelled $\psi = 0$, while the lower boundary typically maps to $\psi = -\pi$; consequently the flow region is known completely. The fluid velocity is singular at the points labelled B and C, shown as black circles.

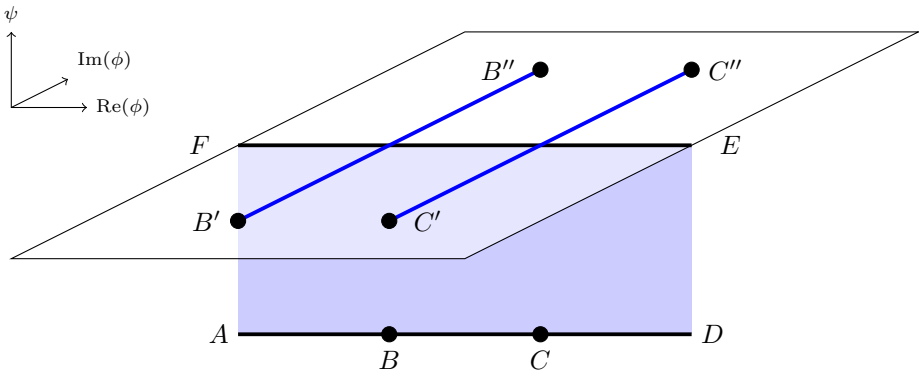

Figure 2: This schematic illustrates the effect of analytically continuing the free surface in the complex potential plane. The analytically continued free surface contains singularities at B', B'', C', and C'', indicated by black circles. These singularities are located at the same position as the singularities in the flow (and the corresponding complex conjugate location). This is because both potential flow and analytic continuation satisfy Laplace's equation. The singularities in the analytically continued free surface produce Stokes curves, represented by blue lines. Exponentially small waves appear as these curves are crossed.

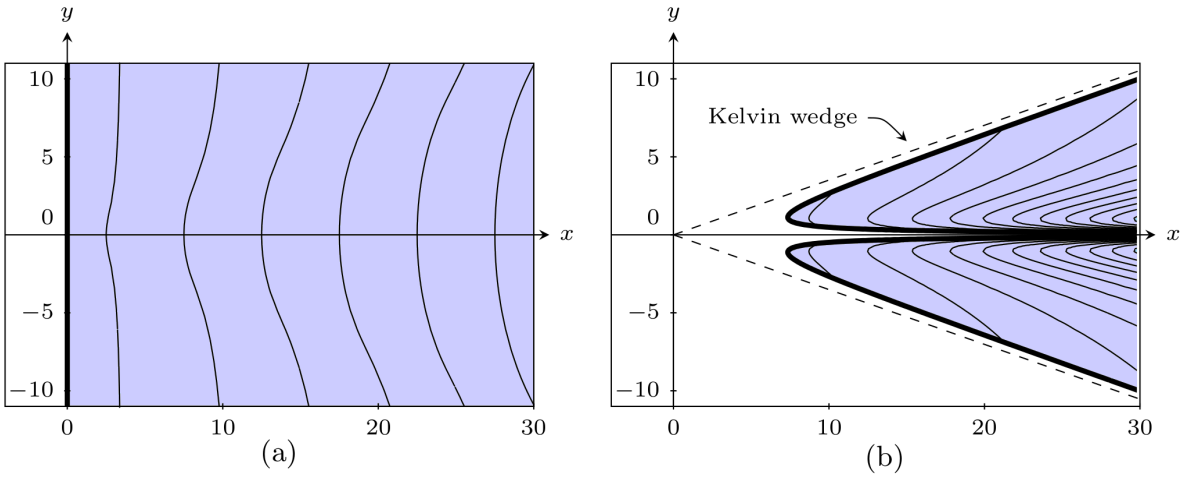

Figure 3: Stokes curves and equal phase lines for surface gravity waves in three dimensional flow past a submerged source propagating in a (a) parallel and (b) perpendicular direction relative to the flow, created using calculations from [29]. Stokes curves are shown as bold curves, while equal phase lines are shown as thin curves. The waves are present in the blue shaded area, with the submerged source located below $(x, y) = (0, 0)$. Transverse waves are located entirely within the Kelvin wedge, while longitudinal waves are propagate outwards, with the amplitude decaying exponentially outside of this wedge.

and the method of steepest descents more directly [45].

One important question left open by [15, 16] was whether exponential asymptotics could incorporate both surface tension and gravity to study gravity-capillary waves in these geometries. Exponential asymptotics were used in [46, 47] to study the problem of gravity-capillary waves over a submerged obstacle in both linear and nonlinear regimes. These studies found that the interactions between gravity and capillary waves produced a rich variety of behaviour. They identified theoretical waves that had not been previously encountered in numerical studies, due to the challenges involved in simulating a system with upstream propagating capillary waves, and downstream propagating gravity waves.

In addition to two-dimensional geometries, it became apparent that Stokes phenomenon plays an important role in the behaviour of water waves when considering three dimensional geometries. These studies built on work by Keller [26], who used geometric ray theory to study gravity waves caused by flow past a surface obstacle. This approach could not easily be extended to submerged obstacles, as the surface waves are exponentially small in this case. Lustri & Chapman [29] considered steady flow past a submerged obstacle using exponential asymptotic methods, and derived asymptotic expressions for waves on the free surface travelling both perpendicular and parallel to the flow direction. This study found that the surface waves tend to the famous Kelvin wedge as the source moves towards the surface. Figure 3 illustrates the Stokes curves and equal phase lines for (a) parallel and (b) perpendicular waves.

Each of the problems described here involved steady flows, as it was clear that unsteady flows would contain substantially more complicated variants of Stokes switching. Lustri [28] showed that unsteady flows in two dimensions can be studied using exponential asymptotics, and that the time-dependent wave propagation is governed by "higher-order Stokes phenomenon", in which Stokes curves themselves switch on or off across higher-order Stokes curves [14, 25]. This work also used exponential asymptotics to describe transient ripples that are not present in steady variants of this free-surface wave problem. These ideas were extended to three dimensional unsteady waves in [30], in which higher-order Stokes phenomenon explains the formation of both tranverse and longitudinal gravity waves. More recently, steady and unsteady three-dimensional capillary waves were described in [33].

1.2 Exponential Asymptotics

The first step in exponential asymptotic analysis is to express the solution as an asymptotic power series in some limit, say $\epsilon \to 0$. In many singular perturbation problems, the asymptotic series solution diverges. If all

of the series terms are known, it is straightforward to truncate a divergent series can be truncated optimally to provide a useful approximation. Unfortunately, the series terms are frequently intractable beyond the first few terms. In practice, however, one does not require the exact form of the series coefficients. Instead, one needs only an asymptotic expressions for the nth series coefficient in the $n \to \infty$ limit, known as the "late-order terms".

Dingle [17] noted that the terms of the divergent asymptotic power series of a singularly perturbed system are typically obtained by repeated differentiations, and therefore diverge in a predictable factorial-over-power manner. Chapman et al. [13] proposed writing an ansatz for the late-order terms that can capture factorial-over-power divergence. One can write an ansatz for the nth term of a divergent asymptotic series (denoted here as q_n) as $n \to \infty$ using the form

$$q_n \sim \frac{Q\Gamma(kn+\gamma)}{\chi^{kn+\gamma}} \qquad \text{as} \qquad n \to \infty, \tag{1}$$

where Q, γ, and χ are functions that do not depend on n but are free to vary with independent variables, such as z, while k is the number of differentiations required to compute q_n from q_{n-1}. The function χ is the "singulant", and equals zero at particular values of z where the leading-order behavior is singular (denoted here as z_0). It is easy to see that the late-order ansatz for q_n is also singular at $z = z_0$, and that the singularity increases in strength as n increases. In practice, γ typically takes constant value, and we will assume this to be the case in the present study. One can then use this ansatz to optimally truncate the asymptotic expansion. The method developed by Olde Daalhuis et al. [36] involves using this form of the late-order terms to truncate the asymptotic expansion optimally, and then the original problem may be rescaled to obtain an equation for the exponentially small remainder term.

In general, the exponentially small contribution to the asymptotic solution that one obtains using the above method, denoted q_{exp}, generally takes the form

$$q_{\text{exp}} \sim \mathcal{S} F \, \mathrm{e}^{-\chi/\epsilon} \qquad \text{as} \qquad \epsilon \to 0, \tag{2}$$

where the "Stokes multiplier" $\mathcal{S}$ varies rapidly from zero to a nonzero constant a Stokes curve is crossed. This behaviour, known as "Stokes switching", is precisely what Stokes identified in his study of the Airy function. It occurs along curves at which the switching exponential is maximally subdominant, and hence where the singulant χ is real and positive [17].

2 Flow past an elastic sheet

2.1 Formulation

In this paper, we adapt the analysis of [15] in order to study surface waves caused by flow past a submerged step with angle β, under an elastic sheet. We assume the sheet to be infinitely thin. This produces the same fluid equations as the previous analysis, but a different boundary condition on the free surface. The configuration is illustrated in Figure 1 (a).

In the fluid region, we consider irrotation, incompressible, inviscid flow past an inclined step of angle β. We may therefore define a velocity potential ϕ such that the fluid velocity is given by $\boldsymbol{u} = (u, v) = \boldsymbol{\nabla}\phi$, and the potential satisfies

$$\boldsymbol{\nabla}^2\phi = 0. \tag{3}$$

At the free surface the velocity potential must satisfy Bernoulli's equation for inviscid flow

$$\frac{1}{2}|\boldsymbol{\nabla}\phi|^2 - \frac{1}{2} + \frac{p}{\rho} = 0, \tag{4}$$

where p is the pressure on the fluid from the elastic sheet and ρ is the density of the fluid. The two dimensional energy per unit length for an inextensible elastic sheet is proportional to the curvature of the sheet squared [4] and so the pressure on the fluid is related to the curvature through

$$p = \sigma\kappa_{ss} \tag{5}$$

where σ is a material constant, κ is the signed curvature, positive if the centre of curvature lies in the fluid region, and s is the arc length along the surface. It is straightforward to non-dimensionalise this system to give

$$\frac{1}{2}|\boldsymbol{\nabla}\phi|^2 - \frac{1}{2} = -\epsilon^3 \kappa_{ss}, \tag{6}$$

where ϵ is a non-dimensional elasticity parameter. We are interested in the regime $0 < \epsilon \ll 1$, corresponding to low rigidity. This surface condition differs to that in [15] through the derivatives of κ in the singularly perturbed term. Consequently, much of the analysis here is very similar to that of the capillary wave problem in the absence of gravity.

A range of models have been used to study elastic sheets on top of a fluid, including the classical Kirchhoff-Love plate model used in [37], or the more recent formulation by Plotnikov and Toland formulation that conserves elastic potential energy [40]. Models describing elastic sheets on fluid are typically extensions of two-dimensional theory derived from the Euler-Bernoulli beam equation. It is therefore unsurprising that in the current two-dimensional geometry with gravity neglected, these models all produce the boundary expression (6), derived from the beam equation [21].

We define the complex potential as $w = \phi + \mathrm{i}\psi$, where ψ is the streamfunction, and we choose the streamfunction to be zero on the free boundary, with the fluid region continuing downwards. The transformation between $z = x + \mathrm{i}y$ and w is a conformal mapping of the flow region. We define a second transformation $w \mapsto \zeta$ where $\zeta = \xi + \mathrm{i}\eta$; this mapping is chosen to transform the flow region to the entire upper half plane. For the specific geometry of flow over an obstacle considered here, the flow domain is restricted to $\psi \in (-\pi, 0]$. We therefore choose $\zeta = \mathrm{e}^w$. The effect of this mapping is shown in Figure 4. The physical free surface maps to $\xi > 0$, while the submerged boundary maps to $\xi < 0$.

As in [15, 16], we work in terms of the complex velocity $\mathrm{d}w/\mathrm{d}z = u - \mathrm{i}v$, written as $q\mathrm{e}^{-\mathrm{i}\theta}$. In this formulation, q is the flow velocity at a point, and θ is the angle the streamlines make with the horizontal axis. Noting that

$$\kappa = \frac{\mathrm{d}\theta}{\mathrm{d}s} \qquad \text{and} \qquad \frac{\mathrm{d}}{\mathrm{d}s} = q\frac{\mathrm{d}}{\mathrm{d}\phi}, \tag{7}$$

Bernoulli's condition (6) on the free boundary becomes

$$q^2 - 1 = -2\epsilon^3 \left[q\left(\frac{\mathrm{d}q}{\mathrm{d}\phi}\right)^2 \frac{\mathrm{d}\theta}{\mathrm{d}\phi} + q^2 \frac{\mathrm{d}\theta}{\mathrm{d}\phi}\frac{\mathrm{d}^2 q}{\mathrm{d}\phi^2} + 3q^2 \frac{\mathrm{d}q}{\mathrm{d}\phi}\frac{\mathrm{d}^2\theta}{\mathrm{d}\phi^2} + q^3 \frac{\mathrm{d}^3\theta}{\mathrm{d}\phi^3}\right]. \tag{8}$$

We will specify the submerged boundary conditions in the ζ-plane for simplicity, given by

$$\theta = \begin{cases} 0 & \xi < -b \\ \beta & -b < \xi < -a \\ 0 & -a < \xi < 0 \end{cases} \tag{9}$$

Now, as the map $w \mapsto \zeta$ is conformal, the behaviour of the surface is given by the integral equation

$$\begin{aligned} \log q &= -\frac{1}{\pi} \fint_{-\infty}^{\infty} \frac{\theta(s)\,\mathrm{d}s}{s - \xi}, \\ &= -\frac{\beta}{\pi} \log\left(\frac{\xi + a}{\xi + b}\right) - \frac{1}{\pi} \fint_0^{\infty} \frac{\theta(s)\,\mathrm{d}s}{s - \xi}. \end{aligned} \tag{10}$$

As both analytic continuation and potential flow are governed by Laplace's equation. We may therefore analytically continue the free surface behaviour simply by replacing ϕ with w in the boundary condition (8), as long as we are careful to interpret w as the position on the analytically continued free surface, rather than within the flow region. The equations governing the analytically continued free surface behaviour are therefore given by

$$q^2 - 1 = -2\epsilon^3 \left[q\left(\frac{\mathrm{d}q}{\mathrm{d}w}\right)^2 \frac{\mathrm{d}\theta}{\mathrm{d}w} + q^2 \frac{\mathrm{d}\theta}{\mathrm{d}w}\frac{\mathrm{d}^2 q}{\mathrm{d}w^2} + 3q^2 \frac{\mathrm{d}q}{\mathrm{d}w}\frac{\mathrm{d}^2\theta}{\mathrm{d}w^2} + q^3 \frac{\mathrm{d}^3\theta}{\mathrm{d}w^3}\right], \tag{11}$$

$$\log q - \mathrm{i}\theta = -\frac{\beta}{\pi} \log\left(\frac{\zeta + a}{\zeta + b}\right) - \frac{1}{\pi} \int_0^{\infty} \frac{\theta(s)\,\mathrm{d}s}{s - \zeta}. \tag{12}$$

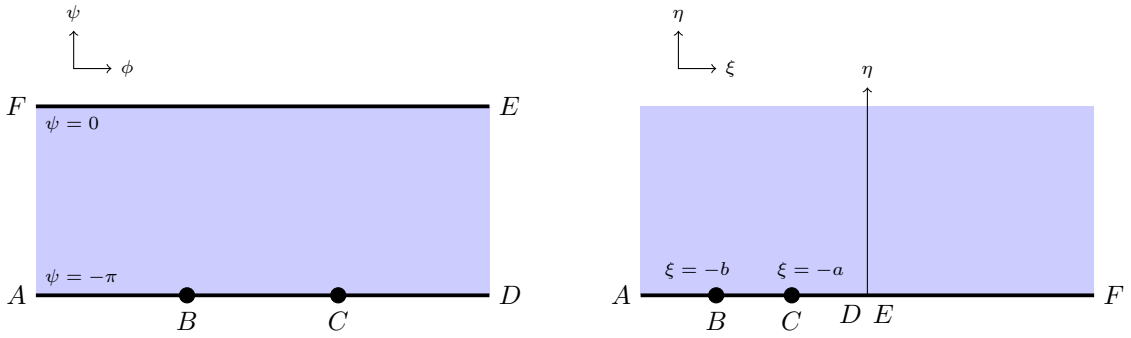

(a) Complex Potential Domain: $w = \phi + \mathrm{i}\psi$ (b) Mapped Fluid Domain: $\zeta = \xi + \mathrm{i}\eta$

Figure 4: This schematic illustrates the effect of the mapping $w \mapsto \zeta$ between the fluid potential domain, shown in (a), and the mapped domain, shown in (b). The mapping takes the fluid region to the entire upper half mapped plane. The free surface $\psi = 0$ maps to the line $\xi > 0$, and the submerged boundary $\psi = -\pi$ maps to the line $\xi < 0$. The singularities map to points which will be labelled $\zeta = -b$ and $\zeta = -a$.

2.2 Asymptotic Power Series

The first step to finding the wave behaviour on the surface of the flow is to expand the solution in terms of an asymptotic power series,

$$q \sim \sum_{n=0}^{\infty} \epsilon^{3n} q_n, \qquad \theta \sim \sum_{n=0}^{\infty} \epsilon^{3n} \theta_n. \tag{13}$$

Substituting these series into (11)–(12) and matching at $\mathcal{O}(1)$ as $\epsilon \to 0$ gives

$$q_0 = 1, \qquad \theta_0 = \frac{\beta}{\pi}\left[\arctan(\sqrt{\zeta/b}) - \arctan(\sqrt{\zeta/a})\right]. \tag{14}$$

The expression for θ_0 is singular at $z = -b$ and $z = -a$. As this problem is singularly perturbed, Stokes curves in the solution are generated at these singular points.

We can obtain expressions for subsequent terms in the series by matching at higher orders of ϵ as $\epsilon \to 0$. It is straightforward to see that $q_1 = -\theta_0'''$. Continuing this process gives the recurrence relation for $n \geq 2$

$$2q_0 q_n = -2\frac{\mathrm{d}\theta_0}{\mathrm{d}\zeta}\frac{\mathrm{d}^2 q_{n-1}}{\mathrm{d}\zeta^2} - 2\frac{\mathrm{d}^3\theta_{n-1}}{\mathrm{d}\zeta^3} + \ldots, \tag{15}$$

$$\frac{q_n}{q_0} - \frac{q_{n-1}q_1}{q_0^2} + \ldots - \mathrm{i}\theta_n = -\frac{1}{\pi}\int_0^{\infty} \frac{\theta_n(s)\,\mathrm{d}s}{s - \zeta}, \tag{16}$$

where the omitted terms are subdominant in the limit that $n \to \infty$ compared to those that have been retained, and are therefore not required for this analysis. Specifically, each of the omitted terms can be shown to be $\mathcal{O}(q_{n-1}')$ in the limit that $n \to \infty$.

2.3 Late-Order Terms

In principle, the recursion relation (15)–(16) could be repeatedly applied in order to obtain terms in the series up to arbitrarily large values of n, given all previous terms in the series. This would be technically challenging, and would not reveal the behaviour of the exponentially small waves, as an asymptotic power series is unable to express behaviour that occurs on these scales.

Instead, we follow [13] and write a factorial-over-power ansatz for the asymptotic terms in the limit that $n \to 0$, with a similar form to (1). By inspecting the recurrence relation, it is clear that obtaining q_n requires differentiating θ_{n-1} three times. Consequently, we expect the strength of singularities in the analytically continued solution to increase by three at each order. Motivated by this observation, we pose the ansatz

$$q_n \sim \frac{Q\Gamma(3n+\gamma)}{\chi^{3n+\gamma}}, \qquad \theta_n \sim \frac{\Theta\Gamma(3n+\gamma)}{\chi^{3n+\gamma}}, \qquad \text{as} \qquad n \to \infty, \tag{17}$$

where Q and χ are functions of w, γ is a constant, and $\chi = 0$ at singular points in θ_0, located at $w = -\log(a) - \mathrm{i}\pi$ and $w = -\log(b) - \mathrm{i}\pi$. We denote these singular points as w_a and w_b respectively.

At this stage we note that for sufficiently large n, the terms of the asymptotic series grow rapidly as n increases. Consequently, $q_n \gg q_{n-k}$ and $\theta_n \gg \theta_{n-k}$ as $n \to \infty$, with the size being controlled by the argument of the gamma function. It is this observation that allows us to omit terms that are $\mathcal{O}(q'_{n-1})$ in the recurrence relation (15)–(16). We may also ignore the effects of the right-hand side integral in (16). This integral plays an important role at early orders, but does not contribute to the late-order expressions; see [48] a more detailed discussion of this technical point.

Applying the late-order ansatz to the recurrence relation (15)–(16) and matching at leading order, or $\mathcal{O}(q_n)$ as $n \to \infty$, gives

$$2Q = -2(-\chi')^3\Theta, \tag{18}$$

$$Q - \mathrm{i}\Theta = 0, \tag{19}$$

where we use $'$ to denote differentiation with respect to w. This gives $Q = \mathrm{i}\Theta$, and can be solved to find χ. Recalling that χ must be zero at singular points in the leading order expression for θ, we write

$$\chi' = -\mathrm{i}, \qquad \chi' = \pm\frac{\sqrt{3}}{2} - \frac{\mathrm{i}}{2}, \tag{20}$$

where θ_0 is singular at $w = w_s$. This shows that, unlike the capillary wave problem, there are three exponentially small wave contributions; however, from the form of (2), we conclude that any exponential term where χ' has nonzero real component must decay exponentially as the distance from the obstacle increases. Consequently, the non-decaying wavetrain must arise due to the singulant contribution given by $\chi' = -\mathrm{i}$. Hence, we only consider

$$\chi = -\mathrm{i}(w - w_s). \tag{21}$$

Matching (15) at the next order, or $\mathcal{O}(q''_{n-1})$ as $n \to \infty$, gives

$$0 = \mathrm{i}\theta_0'\Theta + 3\Theta', \tag{22}$$

which has solution

$$\Theta = \Lambda \mathrm{e}^{-\mathrm{i}\theta_0/3}, \tag{23}$$

where Λ is a constant to be determined. The late-order terms are therefore given by

$$q_n \sim \frac{\mathrm{i}\Lambda \mathrm{e}^{-\mathrm{i}\theta_0/3}\Gamma(3n+\gamma)}{[-\mathrm{i}(w-w_0)]^{3n+\gamma}}, \qquad \theta_n \sim \frac{\Lambda \mathrm{e}^{-\mathrm{i}\theta_0/3}\Gamma(3n+\gamma)}{[-\mathrm{i}(w-w_0)]^{3n+\gamma}}. \tag{24}$$

2.3.1 Determining γ

To determine γ and Λ, we must consider the behaviour of the solution near the singular points $w = w_s$. Near the a corner with in-fluid angle β, the flow behaviour is given by

$$\theta_0 \sim \frac{\mathrm{i}(k-1)}{k}\log(w - w_s), \qquad k = \frac{\pi}{\beta}. \tag{25}$$

Hence, near the singularity, the late-order terms in (23) have the form

$$q_n \sim \frac{\mathrm{i}\Lambda(w-w_s)^{(k-1)/3k}\Gamma(3n+\gamma)}{[-\mathrm{i}(w-w_s)]^{3n+\gamma}}, \qquad \theta_n \sim \frac{\Lambda(w-w_s)^{(k-1)/3k}\Gamma(3n+\gamma)}{[-\mathrm{i}(w-w_s)]^{3n+\gamma}}, \qquad \text{as} \qquad w \to w_s. \tag{26}$$

Recall that the strength of the singularity increases by three at each order. In order for this to be consistent with the leading order logarithmic singularity, we require that the late-order terms have zero singularity strength when $n = 0$. This ensures that the algebraic expression for the late-order terms will have a singularity of order three when $n = 1$, which is consistent with the strength of the singularities in q_1, and so on. In order for this to be the case, we require that $(k-1)/3k - \gamma = 0$, or

$$\gamma = \frac{k-1}{3k}. \tag{27}$$

For a the base of a vertical step, the flow has an in-fluid angle of $\pi/2$, giving $k = 2$ and $\gamma = 1/6$. At the top of a vertical step, the flow has an in-fluid angle of $3\pi/2$, and therefore $k = 2/3$ and $\gamma = -1/6$.

2.3.2 Determining Λ

By comparing (24) with (13), it is clear that the series fails to be asymptotic for w sufficiently close to these singular points. The asymptoticity of the series breaks down when $w - w_s = \mathcal{O}(\epsilon)$ as $\epsilon \to 0$. Computing Λ requires matching the outer behaviour of the late-order terms with an rescaled inner expansion in the neighbourhood of the singularity. This is a technical procedure which will only be outlined here.

We define a new inner variable $\epsilon\eta = -\mathrm{i}(w - w_0)$. Using a very similar approach to [15], we express (25) in terms of inner coordinates and differentiate. This gives

$$\frac{q'}{q} - \mathrm{i}\theta = \frac{k-1}{k\eta}, \tag{28}$$

where $'$ now denotes differentiation with respect to η. Expressing the Bernoulli condition (11) in terms of inner coordinates gives

$$q^2 - 1 = -2\left[q(q')^2\theta' + q^2\theta' q'' + 3q^3 q'\theta'' + q^3\theta'''\right]. \tag{29}$$

The expression in (28) may be applied to this equation to eliminate θ. By setting

$$q \sim \sum_{n=0}^{\infty} \frac{A_n}{\eta^{3n}}, \tag{30}$$

we can match with the inner limit of the outer solution to obtain

$$\mathrm{i}^{\gamma+1}\Lambda = \lim_{n\to\infty} \frac{A_n}{\Gamma(3n+\gamma)}. \tag{31}$$

We note that Λ does not tend to the a constant with the same magnitude for the top of a step as the base, unlike the capillary wave problem. Consequently, we do not expect there to be special values of the step which eliminate waves entirely. For example, if the step is vertical, we find that the bottom angle satisfies $\Lambda \approx -0.615\mathrm{i}^{5/6}$, while the top angle satisfies $\Lambda \approx 0.401\mathrm{i}^{7/6}$. We will explore the impact of this in Section 3.

2.4 Stokes curves

The general form of the late-order terms is given by (24), with γ given in (27) and Λ given in (31). One advantage of this method is that the late-order terms can be used to determine the Stokes structure of the system directly. In Section 1.2, it was noted that Stokes curves follow curves where the exponential is maximally subdominant compared to the base flow; these curves correspond to $\mathrm{Im}(\chi) = 0$ and $\mathrm{Re}(\chi) > 0$.

In the elastic sheet system, we have two singularities in the analytically continued leading order behaviour, corresponding to the base of the step at $w = -\log(a) - \mathrm{i}\pi$, labelled w_a, and $w = -\log(b) - \mathrm{i}\pi$, labelled w_b. We therefore have two singulants to consider, which we will denote

$$\chi_a = -\mathrm{i}(w - w_a), \qquad \chi_b = -\mathrm{i}(w - w_b). \tag{32}$$

We must decide on which side of the Stokes curves the waves are present. For simplicity, we make the same choice as [15] and enforce that the flow is asymptotically flat upstream, and therefore all waves appear downstream from the disturbance. Using this information, we determine the Stokes structure in the solution, presented in Figure 5.

From this figure, it is apparent that there are no wave contributions in the upstream region of the free surface. The first Stokes curve intersects the free surface at $\phi = -\log(b)$, and switches on one exponentially small wave contribution as it is crossed towards the downstream region. The second Stokes curve intersects the free surface at $\phi = -\log(a)$, and a second wave contribution is switched on as it is crossed. The combined effect of this Stokes switching is that the far downstream region contains two exponentially small wave contributions.

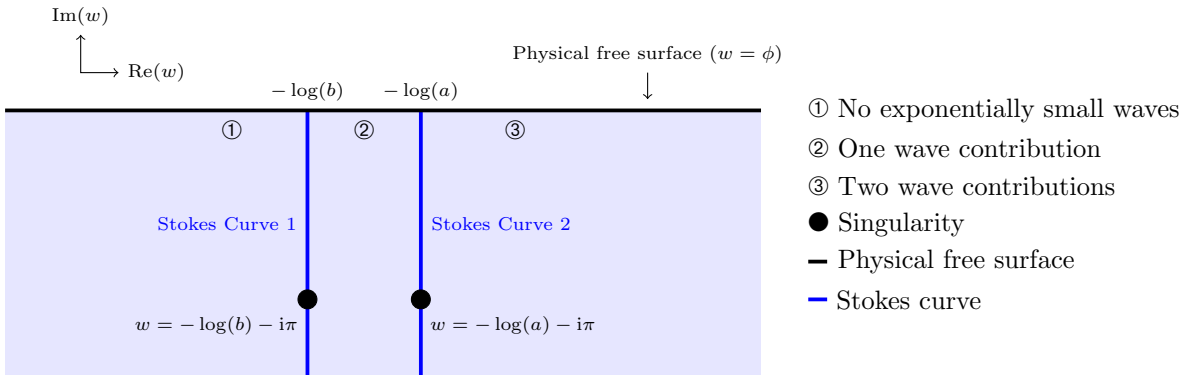

Figure 5: This schematic shows the location of singularities in the analytically continued free surface, represented as black circles. Stokes curves emerge from these singularities and intersect the physical free surface at $\phi = -\log(b)$ and $\phi = -\log(a)$. The Stokes curves divide the physical free surface into three regions. Region ① corresponds to the asymptotically flat upstream region. As the first Stokes curve is crossed into Region ②, one wave contribution is switched on. As the second Stokes curve is crossed into Region ③, a second wave contribution appears. The downstream region therefore contains exponentially small wave contributions from both singularities in the analytically continued free surface.

2.5 Stokes curve analysis

It is straightforward to use the late-order terns from (24) to calculate the amplitude of the waves using the matched asymptotic expansion method of [36]. We will optimally truncate the asymptotic series in (13), and rescale to study the exponentially small remainder in the neighbourhood of the Stokes lines. This will reveal the form of the contribution switched across the Stokes curves. As method is nearly identical to many previous examples, including [15, 16], we will therefore present this section in a brief fashion.

Truncating (13) gives

$$\theta = \sum_{n=0}^{N-1} \epsilon^{3n}\theta_n + R_N, \qquad q = \sum_{n=0}^{N-1} \epsilon^{3n} q_n + S_N. \tag{33}$$

Boyd [11] gives a heuristic for finding the optimal truncation point of a divergent series, which is to find the value of N that minimises the magnitude of the series terms . For this problem, this gives $N \sim |\chi|/3\epsilon$. We therefore set $N = |\chi|/3\epsilon + \omega$, where $\omega \in [0, 1)$ in order to truncate at an integer value. Applying the the truncated series to (11)–(12) gives, after some simplification,

$$\mathrm{i}R_N + \epsilon^3 \left(\frac{\mathrm{d}^3 R_N}{\mathrm{d}w^3} + \mathrm{i}\frac{\mathrm{d}\theta_0}{\mathrm{d}w}\frac{\mathrm{d}^2 R_N}{\mathrm{d}w^2} \right) \sim \mathrm{i}\epsilon^{3N}\theta_N. \tag{34}$$

Away from the Stokes curve, the right-hand side is smaller than the remainder, and can be neglected. In this case, a Green-Liouville (or WKB) ansatz gives the form of the remainder as $R_N \sim C\Theta \mathrm{e}^{-\chi/\epsilon}$, where C is some undetermined constant. To incorporate the Stokes switching into this expression, we set

$$R_N = \mathcal{S}\Theta \mathrm{e}^{-\chi/\epsilon}, \tag{35}$$

where $\mathcal{S}$ is constant away from the Stokes curve, but varies rapidly in its neighbourhood. This term therefore captures the effect of Stokes switching in the solution. Substituting this expression into (34) gives

$$\frac{\mathrm{d}\mathcal{S}}{\mathrm{d}w} \sim -\frac{\mathrm{i}\epsilon^{3N-1}\Gamma(3N+\gamma)}{\chi^{3N+\gamma}}. \tag{36}$$

Writing the expression in terms of the independent variable χ, setting $\chi = r\mathrm{e}^{\mathrm{i}\vartheta}$ and simplifying gives

$$\frac{\mathrm{d}\mathcal{S}}{\mathrm{d}\vartheta} \sim \frac{\mathrm{i}\sqrt{2\pi r}}{\epsilon^{\gamma+1/2}} \exp\left(\frac{r}{\epsilon}(1 - \exp^{\mathrm{i}\vartheta}) + \mathrm{i}\vartheta(1 - 3\alpha - \gamma) \right) \tag{37}$$

where Stirling's formula was used to simplify the gamma function on the numerator [18]. To examine the behaviour of the remainder near the Stokes curve, we set $\vartheta = \epsilon^{1/2}\hat{\vartheta}$, and obtain the inner expression

$$\frac{\mathrm{d}\mathcal{S}}{\mathrm{d}\hat{\vartheta}} \sim \frac{\mathrm{i}\sqrt{2\pi r}}{\epsilon^{\gamma}} \mathrm{e}^{-r\hat{\vartheta}^2/2}. \tag{38}$$

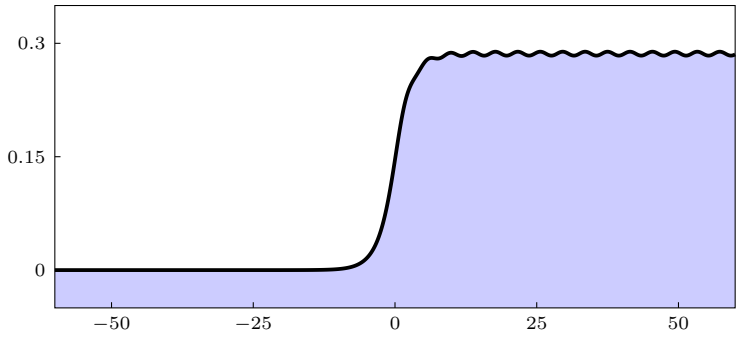

Figure 6: Numerically computed free surface for flow from left to right over a vertical step with $a = 1$, $b = 1.25$, and $\epsilon = 0.63$. Exponentially small waves are visible on the downstream surface of the flow

Solving this expression gives

$$\mathcal{S} \sim \lambda + \frac{\pi \mathrm{i}}{\epsilon^{\gamma}} \mathrm{erf}\left(\frac{\sqrt{r}\hat{\vartheta}}{\sqrt{2}}\right), \tag{39}$$

where λ is a constant to be determined. The downstream outer region corresponds to the limit that $\hat{\vartheta} \to -\infty$, while the upstream region corresponds to $\hat{\vartheta} \to \infty$. We therefore we enforce the condition that the flow is wave-free far upstream by requiring that $\mathcal{S}$ tends to zero in the limit that $\hat{\vartheta} \to \infty$. This gives $\lambda = -\pi \mathrm{i}/\epsilon^{\gamma}$.

Hence, in the downstream region (obtained by taking the limit $\hat{\vartheta} \to -\infty$), we find that

$$\mathcal{S} \sim -\frac{2\pi \mathrm{i}}{\epsilon^{\gamma}}. \tag{40}$$

Therefore the oscillatory behaviour switched on as the Stokes line is crossed from upstream to downstream is given by

$$R_N \sim -\frac{2\pi \mathrm{i}\Theta}{\epsilon^{\gamma}} \mathrm{e}^{-\chi/\epsilon}. \tag{41}$$

The full exponentially small contribution to the solution behaviour is obtained by computing the remainder (41) associated with both of the singularities depicted in Figure 5. Furthermore, analytically continuing the fluid flow upwards rather than downwards in the formulation generates two complex conjugate contributions. Hence, the full exponentially small behaviour downstream from the obstacle is given by

$$\theta_{\mathrm{exp}} \sim -\frac{2\pi \mathrm{i}\Lambda_a \mathrm{e}^{-\mathrm{i}\theta_0/3}}{\epsilon^{\gamma_a}} \mathrm{e}^{-\pi/\epsilon} \mathrm{e}^{-\mathrm{i}(\phi + \log(a))/\epsilon} - \frac{2\pi \mathrm{i}\Lambda_b \mathrm{e}^{-\mathrm{i}\theta_0/3}}{\epsilon^{\gamma_b}} \mathrm{e}^{-\pi/\epsilon} \mathrm{e}^{-\mathrm{i}(\phi + \log(b))/\epsilon} + \mathrm{c.c.}, \tag{42}$$

where we have converted back into the original potential coordinate ϕ.

The variation in the physical flow region is obtained by integrating this expression with respect to ϕ. Adding the complex conjugate contributions gives

$$y_{\mathrm{exp}} \sim 4\pi\epsilon \mathrm{e}^{-\pi/\epsilon} \mathrm{Re}\left[\mathrm{e}^{-\mathrm{i}\theta_0/3}\left(\frac{\Lambda_a}{\epsilon^{\gamma_a}} \mathrm{e}^{-\mathrm{i}(\phi + \log(a))/\epsilon} + \frac{\Lambda_b}{\epsilon^{\gamma_b}} \mathrm{e}^{-\mathrm{i}(\phi + \log(b))/\epsilon}\right)\right]. \tag{43}$$

We note that, far downstream from the obstacle, this expression can be simplified further by noting that $\theta_0 \to 0$ as $\phi \to \infty$.

3 Results

In the previous section, we computed the exponentially small variation in angle (42), and hence the free surface position (43) downstream from the submerged obstacle. This expression is the sum of two exponentially small wavetrains, each of which switch across a different Stokes curve. In order to confirm this asymptotic prediction, we compare it to numerical free surface simulations of the system (8)–(10).

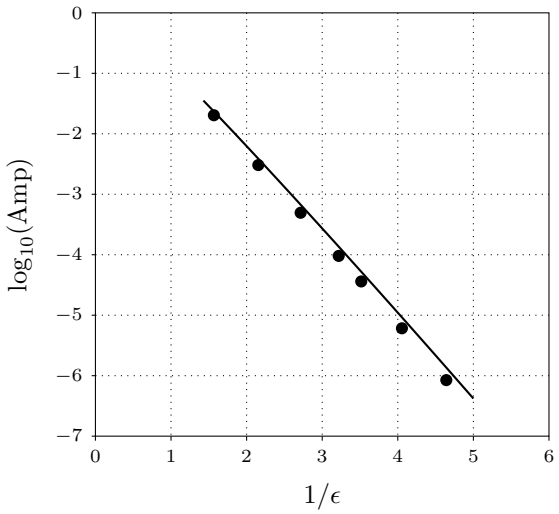

Figure 7: Logarithm of the amplitude of the downstream elastic waves over a vertical step with $a = 1$ and $b = 2$, as a function of $1/\epsilon$. The filled circles represent sample numerical solutions, while the solid curve shows the asymptotic prediction for the amplitude. The numerics confirm the accuracy of the asymptotic approximation.

The numerical method used here is described in detail in [39], and uses a Jacobian-free Newton-Krylov method to solve the full nonlinear system. The free surface is truncated and discretised using 6001 grid points in the domain $\phi \in [-50, 50]$. The upstream region is prescribed to be waveless, and given unit flow velocity. The governing equations (8) and (10) are then evaluated at each point to form a system of nonlinear equations that are solved using using a Newton-like iteration with preconditioning.

From this system, we obtain the amplitude of the elastic waves. In Figure 6, we present a sample free surface in which the elastic waves are visible in the downstream region. This surface corresponds to $\epsilon = 0.63$, with $a = 1$ and $b = 1.25$. While this is not a particularly small value of ϵ, it is chosen as a representative example in order for the downstream waves to be easily visible in the figure.

It is not possible to distinguish the two different Stokes switching contributions in Figure 6, as the Stokes curves intersect the free surface at $\phi = 0$ and $\phi \approx -0.22$, corresponding to points that are relatively close in the physical plane. For larger values of b, the intermediate region could possibly be distinguished; however, increasing b increases the computational difficulty of solving the nonlinear system for the boundary behaviour using the method described here.

In Figure 7, we compare these computations to the downstream amplitude predicted by this analysis for a step with angle $\pi/2$, with $a = 1$ and $b = 2$, for a range of ϵ. It is clear that there is strong agreement between the numerical and asymptotic predictions of the elastic wave behaviour.

4 Discussion

We presented this short note for two purposes. The first purpose of this note was to highlight the important role played by Stokes phenomenon in the study of water waves. In recent years, research has revealed that water waves in singularly perturbed systems are frequently a consequence of Stokes Phenomena. By studying the behaviour of Stokes curves, it is possible to understand a wide range of water wave behaviour, including flow past obstacles, as well as waves in more complicated flow configurations such as gravity-capillary waves, unsteady waves, or waves in three dimensions.

The second purpose of this note was to briefly present a new result regarding flow past obstacles underneath an elastic sheet. In many respects, this problem is very similar to the problem of capillary waves caused by flow past an obstacle considered in [15]. While much of the mathematics is similar, it is hoped that this problem can highlight that the utility of Stokes phenomenon in fluid dynamics problems is not solely limited to the study of classical water waves, but that it can provide insight into a wider range of related problems.

In this study, we found that flow past an inclined step under an elastic sheet generates exponentially small waves on the sheet. The downstream region contains two wavetrains; one generated by a singularity in the flow field at the base of the step, and one by a singularity in the flow field at the top of the step. This behaviour was also seen in the study of capillary waves in [15]. Unlike this previous work, however, the elastic sheet problem does not have a set of configurations for which the waves cancel completely.

This study raises a number of interesting questions which we hope will inspire further study into these elastic waves. While a single step cannot produce wave cancellation, it is possible that more complicated geometries such as ridges or trenches may lead to trapped wave configurations, as in [31]. It is known that a variety of wave behaviour can be obtained by including compressive stress in the elastic sheet (see, for example, [5]), and it would be interesting to explore these effects in the context of flow over an obstacle.

In [15, 16], it was shown that the gravity and capillary waves arise in the linear problem obtained by linearising around a small step height. This provided an avenue to study these waves in three dimensions using linear theory [29, 30, 33]. While we did not consider the linearized elastic sheet problem here, the wave behaviour in this problem can be obtained using a method similar to the corresponding analysis in [15]. This suggests that it is possible to study elastic waves in a linearized three-dimensional regime, in which the waves typically arise due to Airy-type behaviour in the analytically-continued complex domain.

Many of the most interesting questions regarding waves in elastic sheets arise in the study of flexural-gravity waves; that is, including the effects of gravity. This is the natural next step to explore using exponential asymptotic methods. Given the similarity between gravity-capillary and flexural-gravity waves, it is likely that an analysis of this sort would share many similarities with the gravity-capillary studies of Trinh & Chapman [46, 47]. Implementing a computational scheme for the full nonlinear flexural-gravity wave problem would be challenging due to the fact that the different wave contributions propagate in opposite directions (as in the gravity-capillary problem, discussed in detail in [47]), making numerical studies more complicated.

5 Acknowledgements

CJL acknowledges the support of ARC Discovery Project DP190191190, and Macquarie University Seeding Grant 72585747. LK acknowledges the support of ARC Discovery Early Career Research Award DE200100168. RP acknowledges the support of ARC Discovery Project DP180103260. CJL and LK thank Charles Hadeed for valuable discussions about the behaviour of elastic sheets on a flow.

References

[1] T. R. Akylas and T.-S. Yang. On short-scale oscillatory tails of long-wave disturbances. *Stud. Appl. Math.*, 94(1):1–20, 1995.

[2] N. Andersson and C. J. Howls. The asymptotic quasinormal mode spectrum of non-rotating black holes. *Classical Quant. Grav.*, 21(6):1623, 2004.

[3] I. Aniceto, R. Schiappa, and M. Vonk. The resurgence of instantons in string theory. *Commun. Number Theory*, 6(2):339–496, 2012.

[4] B. Audoly and Y. Pomeau. *Elasticity and Geometry: From hair curls to the non-linear response of shells*. OUP Oxford, 2010.

[5] N. J. Balmforth and R. V. Craster. Ocean waves and ice sheets. *J. Fluid Mech.*, 395:89–124, 1999.

[6] M. V. Berry. Stokes phenomenon; smoothing a Victorian discontinuity. *Pub. Math. de L'IHÉS*, 68:211–221, 1988.

[7] M. V. Berry. Uniform asymptotic smoothing of Stokes's discontinuties. *Proc. Roy. Soc. Lond.* A, 422(1862):7–21, 1989.

[8] M. V. Berry. Asymptotics, superasymptotics, hyperasymptotics. In H. Segur, S. Tanveer, and H. Levine, editors, *Asymptotics Beyond All Orders*, pages 1–14. Plenum, Amsterdam, 1991.

[9] M. V. Berry and C. J. Howls. Hyperasymptotics. *Proc. Roy. Soc. Lond.* A, 430(1880):653–668, 1990.

[10] M. V. Berry and C. J. Howls. Hyperasymptotics for integrals with saddles. *Proc. Roy. Soc. Lond.* A, 434(1892):657–675, 1991.

[11] J. P. Boyd. The devil's invention: Asymptotic, superasymptotic and hyperasymptotic series. *Acta Appl. Math.*, 56(1):1–98, 1999.

[12] J. G. Byatt-Smith. On the existence of homoclinic and heteroclinic orbits for differential equations with a small parameter. *Eur. J. App. Math.*, 2(2):133–158, 1991.

[13] S. J. Chapman, J. R. King, and K. L. Adams. Exponential asymptotics and Stokes lines in nonlinear ordinary differential equations. *Proc. Roy. Soc. Lond.* A, 454(1978):2733–2755, 1998.

[14] S. J. Chapman and D. B. Mortimer. Exponential asymptotics and Stokes lines in a partial differential equation. *Proc. Roy. Soc. Lond.* A, 461:2385–2421, 2005.

[15] S. J. Chapman and J.-M. Vanden-Broeck. Exponential asymptotics and capillary waves. *SIAM J. Appl. Math.*, 62(6):1872–1898, 2002.

[16] S. J. Chapman and J.-M. Vanden-Broeck. Exponential asymptotics and gravity waves. *J. Fluid Mech.*, 567:299–326, 2006.

[17] R. B. Dingle. *Asymptotic Expansions: Their Derivation and Interpretation.* Academic Press, New York, 1973.

[18] *NIST* Digital Library of Mathematical Functions. http://dlmf.nist.gov/, Release 1.0.22 of 2019-03-15. F. W. J. Olver, A. B. Olde Daalhuis, D. W. Lozier, B. I. Schneider, R. F. Boisvert, C. W. Clark, B. R. Miller and B. V. Saunders, eds.

[19] L. K. Forbes. Surface waves of large amplitude beneath an elastic sheet. Part 1. High-order series solution. *J. Fluid Mech.*, 169:409–428, 1986.

[20] L. K. Forbes. Surface waves of large amplitude beneath an elastic sheet. Part 2. Galerkin solution. *J. Fluid Mech.*, 188:491–508, 1988.

[21] A. G. Greenhill. Wave motion in hydrodynamics (continued). *American J. Math.*, pages 97–112, 1887.

[22] R. Grimshaw. Exponential asymptotics and generalized solitary waves. In H. Steinrück, F. Pfeiffer, F. G. Rammerstorfer, J. Salençon, B. Schrefler, and P. Serafini, editors, *Asymptotic Methods in Fluid Mechanics: Survey and Recent Advances*, volume 523 of *CISM Courses and Lectures*, pages 71–120. Springer Vienna, 2011.

[23] R. Grimshaw and N. Joshi. Weakly nonlocal solitary waves in a singularly perturbed Korteweg-de Vries equation. *SIAM J. Appl. Math.*, 55(1):124–135, 1995.

[24] P. Guyenne and E. I. Părău. Computations of fully nonlinear hydroelastic solitary waves on deep water. *J. Fluid Mech.*, 713:307–329, 2012.

[25] C. J. Howls, P. J. Langman, and A. B. Olde Daalhuis. On the higher-order Stokes phenomenon. *Proc. Roy. Soc. Lond.* A, 460(2121):2285–2303, 2004.

[26] J. B. Keller. The ray theory of ship waves and the class of streamlined ships. *J. Fluid Mech.*, 91(3):465–488, 1979.

[27] M. D. Kruskal and H. Segur. Asymptotics beyond all orders in a model of crystal growth. *Stud. Appl. Math.*, 85:129–181, 1991.

[28] C. J. Lustri. *Exponential asymptotics in unsteady and three-dimensional flows.* PhD thesis, Oxford University, UK, 2013.

[29] C. J. Lustri and S. J. Chapman. Steady gravity waves due to a submerged source. *J. Fluid Mech.*, 732:660–686, 2013.

[30] C. J. Lustri and S. J. Chapman. Unsteady gravity waves due to a submerged source. *Eur. J. App. Math.*, 1:1, 2014.

[31] C. J. Lustri, S. W. McCue, and B. J. Binder. Free surface flow past topography: A beyond-all-orders approach. *Euro. J. Appl. Math.*, 23(4):441–467, 2012.

[32] C. J. Lustri, S. W. McCue, and S. J. Chapman. Exponential asymptotics of free surface flow due to a line source. *IMA J. App. Math.*, 78(4):697–713, 2013.

[33] C. J. Lustri, R. Pethiyagoda, and S. J. Chapman. Three-dimensional capillary waves due to a submerged source with small surface tension. *J. Fluid Mech.*, 863:670–701, 2019.

[34] A. V. Marchenko and V. I. Shrira. Theory of two-dimensional nonlinear waves in liquid covered by ice. *Fluid Dynamics*, 26(4):580–587, 1991.

[35] P. A. Milewski, J.-M. Vanden-Broeck, and Z. Wang. Hydroelastic solitary waves in deep water. *J. Fluid Mech.*, 679:628–640, 2011.

[36] A. B. Olde Daalhuis, S. J. Chapman, J. R. King, J. R. Ockendon, and R. H. Tew. Stokes phenomenon and matched asymptotic expansions. *SIAM J. App. Math.*, 55(6):1469–1483, 1995.

[37] E. I. Părău and F. Dias. Nonlinear effects in the response of a floating ice plate to a moving load. *J. Fluid Mech.*, 460:281–305, 2002.

[38] E. I. Părău and J.-M. Vanden-Broeck. Gravity-capillary and flexural-gravity solitary waves. In *Nonlinear Water Waves*, pages 183–199. Springer, 2019.

[39] R. Pethiyagoda, T. J. Moroney, and S. W. McCue. Efficient computation of two-dimensional steady free-surface flows. *Int. J. Num. Meth. Fluids*, 86(9):607–624, 2018.

[40] P I. Plotnikov and J. F. Toland. Modelling nonlinear hydroelastic waves. *Phil. Trans. Roy. Soc.* A, 369(1947):2942–2956, 2011.

[41] Y. Pomeau, A. Ramani, and B. Grammaticos. Structural stability of the Korteweg-de Vries solitons under a singular perturbation. *Physica* D, 31(1):127–134, 1988.

[42] G. G. Stokes. On the discontinuity of arbitrary constants which appear in divergent developments. *Trans. Cam. Phil. Soc.*, 10:106–128, 1864.

[43] G. G. Stokes. On the discontinuity of arbitrary constants that appear as multipliers of semi-convergent series. *Acta Mathematica*, 26(1):393–397, 1902.

[44] P. H. Trinh. Exponential asymptotics and Stokes line smoothing for generalized solitary waves. In H. Steinrück, F. Pfeiffer, F. G. Rammerstorfer, J. Salençon, B. Schrefler, and P. Serafini, editors, *Asymptotic Methods in Fluid Mechanics: Survey and Recent Advances*, volume 523 of *CISM Courses and Lectures*, pages 121–126. Springer Vienna, 2011.

[45] P. H. Trinh. A topological study of gravity free-surface waves generated by bluff bodies using the method of steepest descents. *Proc. Roy. Soc.* A, 472(2191):20150833, 2016.

[46] P. H. Trinh and S. J. Chapman. New gravity-capillary waves at low speeds. Part 1. Linear geometries. *J. Fluid Mech.*, 724:367–391, 2013.

[47] P. H. Trinh and S. J. Chapman. New gravity-capillary waves at low speeds. Part 2. Nonlinear geometries. *J. Fluid Mech.*, 724:392–424, 2013.

[48] P. H. Trinh and S. J. Chapman. The wake of a two-dimensional ship in the low-speed limit: results for multi-cornered hulls. *J. Fluid Mech.*, 741:492–513, 2014.

[49] P. H. Trinh, S. J. Chapman, and J.-M. Vanden-Broeck. Do waveless ships exist? Results for single-cornered hulls. *J. Fluid Mech.*, 685:413–439, 2011.

[50] J.-M. Vanden-Broeck and E. I. Părău. Two-dimensional generalized solitary waves and periodic waves under an ice sheet. *Phil. Trans. Roy. Soc.* A, 369(1947):2957–2972, 2011.